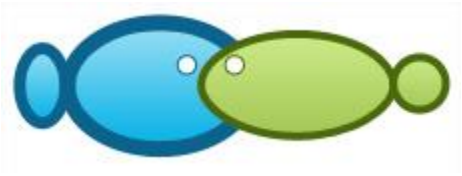

Numerical modeling of debris trajectory in Jakarta Bay: assessing the threat to Seribu Island

[1,2]Mutiara R. Putri, [2]Muhammad Riza, [1]Naffisa A. Fekranie, [3]Agus Setiawan, [4]Hansan Park

[1] Research Group of Environmental and Applied Oceanography, Faculty of Earth Sciences and Technology, Bandung Institute of Technology, Bandung 40132, West Java, Indonesia; [2] Study Program of Earth Science, Faculty of Earth Sciences and Technology, Bandung Institute of Technology, Bandung 40132, West Java, Indonesia; [3] Research Centre for Deep Sea, Research Organisation for Earth Sciences and Maritime, National Research and Innovation Agency, Central Jakarta, Indonesia; [4] Korea-Indonesia Marine Technology Cooperation Research Center (MTCRC), Central Jakarta, Indonesia.
Corresponding author: M. R. Putri, mutiara.putri@itb.ac.id

Abstract. Marine debris poses a significant threat to the health of aquatic ecosystems, particularly those in vulnerable archipelagos like Seribu Island, renowned for its rich coral reef biodiversity. This study investigates the sources and transport patterns of debris originating from rivers flowing into Jakarta Bay, which are suspected to be major contributors to stranded marine debris in the region. Using 3D hydrodynamic and trajectory modeling, the study focuses on debris movement during 2018, particularly the influence of the western and eastern monsoons. The hydrodynamic model results indicate that the average monthly speed of eastward-northeastward surface currents was 0.32 m s^{-1} in January, with the maximum speed occurring in January. Surface currents began to change direction northward in March, with an average speed of 0.26 m s^{-1}. During the eastern monsoon, the average monthly surface currents moved westward at an average speed of 0.27 m s^{-1}, while during the western monsoon, surface currents returned to a westward-northwestward direction at an average speed of 0.25 m s^{-1}. Verification of the trajectory model with field data showed similar movement directions, with a distance difference of no more than 300 m. Excluding local debris sources and mobile sources, the study predicts that the Cengkareng River was a primary source of debris stranding on the islands, with an estimated 4 tons reaching Pramuka Island. Pari Island experienced the highest debris accumulation (4.2 tons) in November, likely originating from multiple rivers including Cisadane, West Flood Channel, and Citarum. The study reveals a decreasing trend in debris amounts from Bidadari Island (closest to Jakarta) to Pramuka Island (furthest north). These findings highlight the critical issue of land-based debris entering marine ecosystems and emphasize the urgent need for effective conservation strategies and legislative measures to address marine debris pollution to protect the aquatic ecosystems of Seribu Island.
Key Words: Cengkareng River, hydrodynamic and trajectory modeling, marine debris, Jakarta Bay, Seribu Island.

Introduction. Jakarta, the capital of Indonesia, is home to 13 rivers originating from Jakarta, Banten, Bogor, and Bekasi, which discharge into the marine waters of Jakarta Bay. These rivers are suspected to be major sources of land-based marine debris. According to the World Bank Group (2018), cities like Jakarta, Banten, and Bekasi are among the most densely populated in Indonesia and significantly contribute to marine waste in Jakarta Bay and the surrounding Java Sea. Additionally, the northern part of Jakarta Bay hosts small islands belonging to the Seribu Island Regency, which have significant marine resource potential for tourism and marine conservation. Pramuka Island, for example, is the capital of the regency, a conservation area, and part of a National Marine Park renowned for its coral reefs, mangroves, and tourism appeal. Transportation facilities and travel times from Jakarta to these islands are convenient for both the public and tourists. Other nearby small islands, such as Tidung Island, Pari Island, Untung Jawa Island, and Bidadari Island, are also easily accessible from Jakarta, enhancing their appeal as tourist destinations.

Seribu Island features diverse ecosystems that support increasing tourism and fishery activities. Wicaksono et al (2022) conducted a study in three locations (Tidung Island, Rambut Island, and PT. Pertamina Plumpang) from May to October 2022 assessing vegetation, fauna, and coral. The diversity index value of flora at PT. Pertamina Plumpang was 3.176, classified as high, with an evenness index of 0.808, also relatively high. The estimated biomass and carbon stock of plant trees at PT. Pertamina Plumpang was 57,314.01 tons ha^{-1}. The percentage of mangrove presence was 33% on Tidung Island and 37% on Rambut Island. The survival rate of coral on Tidung Island was 97%, with a 3% mortality rate. The avifauna composition at PT. Pertamina Plumpang included 12 species from 10 families, with a diversity index value of 1.88 (medium category) and an evenness index value of 0.75 (high value). The herpetofauna composition included 2 species, and 6 insect species were also found.

As marine debris crosses and accumulates in Java Sea (Kisnarti et al 2024), the Seribu Island, located within this sea, is significantly impacted. This ongoing marine debris is likely sourced from the rivers flowing into Jakarta Bay (Diastomo et al 2021; Rahman et al 2024). This was evident in November 2018, when heavy rains in Jakarta caused a massive amount of debris to strand on Pari Island within hours, completely covering its port. This incident demonstrates the vast distances debris can travel and the uncertainty about its origin. This is particularly concerning for Pari Island's ecosystem, which is utilized for tourism (50%), housing (40%), and marine research (10%) (Mulia 2004). Pari Island's coral reef ecosystem, spanning 249.9 hectares across its southern, western, eastern, and northern sides (Widyayanto et al 2009), is a major tourist draw but is threatened by the constant influx of marine debris.

To address this issue, numerical modeling techniques, including hydrodynamic models for obtaining ocean current vectors and particle trajectory models for predicting debris origins, can be employed to investigate the distribution and movement of marine debris in Jakarta Bay (Putri 2005; Mayer & Pohlmann 2014; Putri & Pohlmann 2014; Tsani 2017). Assuming that the debris originates solely from the rivers flowing into Jakarta Bay and not from the islands themselves, this study aims to estimate the source and quantity of debris that became stranded on Seribu Island in November 2018. It also seeks to predict the influence of the western and eastern monsoons on debris distribution from the river estuaries in Jakarta Bay using 3-dimensional hydrodynamic and trajectory modeling.

Material and Method

Model area. Regional Ocean Model Systems (ROMS) was employed for hydrodynamic modeling, utilizing a nested modeling technique. Area A represents the larger model domain, providing input and boundary conditions for the hydrodynamic model in the smaller, more detailed area (Area B) encompassing Jakarta Bay and Seribu Island (Figure 1). Geographically, Area B is situated within coordinates 5°47'49"-6°09'29" S and 106°031'29"-107°02'43" E. Trajectory modeling was restricted to Area B, encompassing the waters of Jakarta Bay extending to Seribu Island.

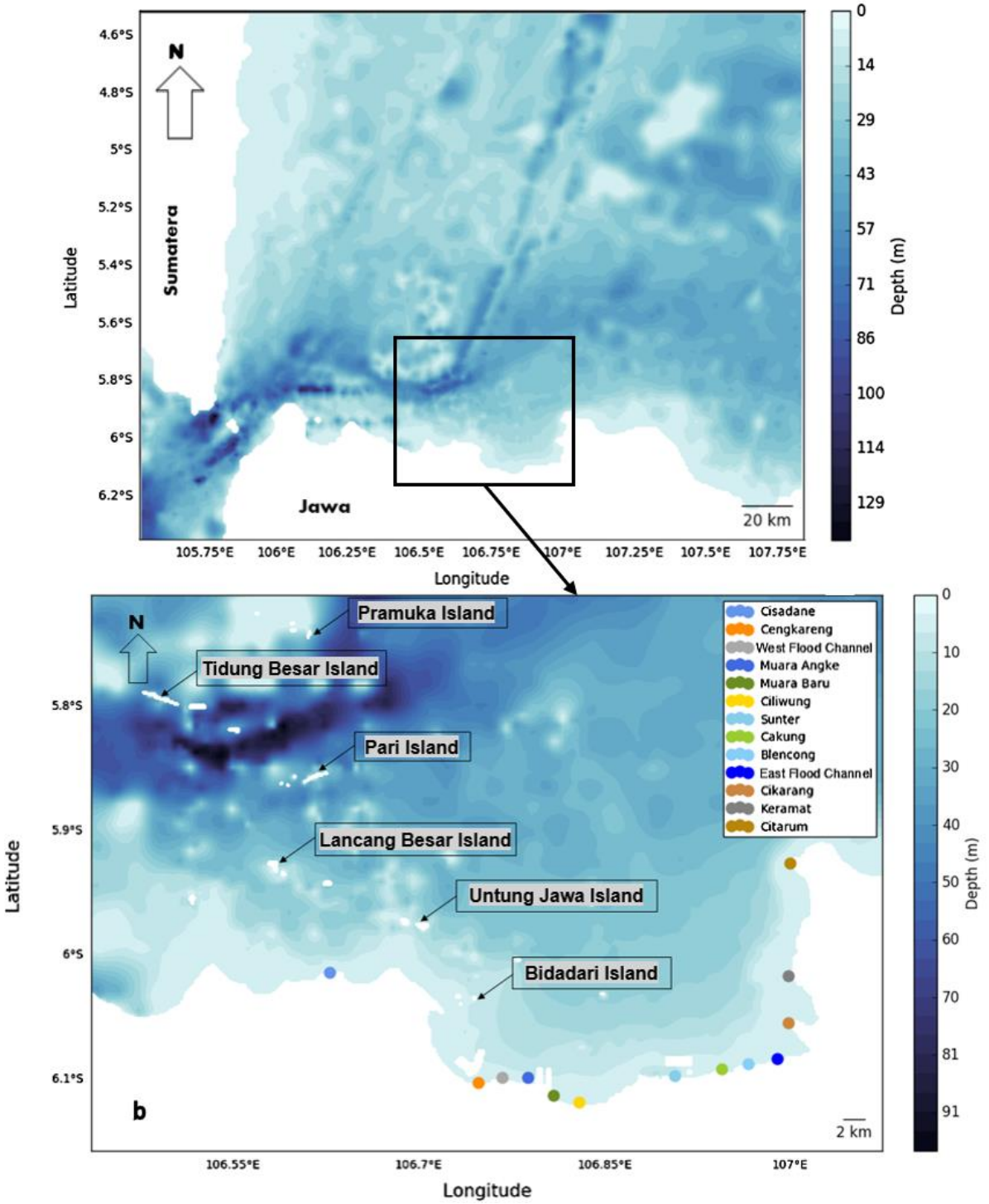

Figure 1. Bathymetry area of (a) large model and (b) small model (detailed) domains. Colored dots represent the 13 river mouths in Jakarta Bay, while black arrows indicate the islands in the Seribu Island.

Model equation. ROMS is a 3-dimensional numerical model that solves the Reynolds-Averaged Navier-Stokes (RANS) equations using the hydrostatic and Boussinesq approximations (Haidvogel & Beckmann 1999; Chassignet et al 2000; Warner et al 2008) with an explicit time-stepping algorithm (Haidvogel & Beckmann 1999; Shchepetkin & McWilliams 2005; Warner et al 2008). ROMS utilizes a curvilinear Arakawa C horizontal grid and a sigma vertical coordinate. Its flexible structure allows for various model component choices, including advection schemes (first-order, second-order, third-order,

and fourth-order), turbulence submodels, and boundary condition variations (Warner et al 2008).

Momentum, scalar advection, and diffusive processes are formulated within transport equations, while density is determined from an equation that accounts for temperature, salinity, and currents. The governing equations are expressed in flux form, using Cartesian horizontal coordinates and sigma vertical coordinates. The momentum equations employed in ROMS are represented by equations (1) and (2), adapted from Warner et al (2008), where the terms u, v, Ω, H_z, f, p, ρ, and g are defined as follows:

x-direction:

$$\frac{\partial(H_z u)}{\partial t} + \frac{\partial(uH_z u)}{\partial x} + \frac{\partial(vH_z u)}{\partial y} + \frac{\partial(\Omega H_z u)}{\partial s} - fH_z v = -\frac{H_z}{\rho_0}\frac{\partial p}{\partial x} - H_z g\frac{\partial \eta}{\partial x} - \frac{\partial}{\partial s}\left(\overline{u'w'} - \frac{v}{H_z}\frac{\partial u}{\partial s}\right) - \frac{\partial(H_z S_{xx})}{\partial x} - \frac{\partial(H_z S_{xy})}{\partial y} - \frac{\partial S_{px}}{\partial s} \quad (1)$$

y-direction:

$$\frac{\partial(H_z v)}{\partial t} + \frac{\partial(uH_z v)}{\partial x} + \frac{\partial(vH_z v)}{\partial y} + \frac{\partial(\Omega H_z v)}{\partial s} + fH_z u = -\frac{H_z}{\rho_0}\frac{\partial p}{\partial y} - H_z g\frac{\partial \eta}{\partial y} - \frac{\partial}{\partial s}\left(\overline{v'w'} - \frac{v}{H_z}\frac{\partial v}{\partial s}\right) - \frac{\partial(H_z S_{yx})}{\partial x} - \frac{\partial(H_z S_{yy})}{\partial y} - \frac{\partial S_{py}}{\partial s} \quad (2)$$

z-direction:

$$0 = -\frac{1}{\rho_0}\frac{\partial p}{\partial s} - \frac{g}{\rho_0}H_z\rho \quad (3)$$

The continuity equation, which represents the conservation of mass, is expressed as follows:

$$\frac{\partial \eta}{\partial t} + \frac{\partial(H_z u)}{\partial x} + \frac{\partial(H_z v)}{\partial y} + \frac{\partial(H_z \Omega)}{\partial s} = 0 \quad (4)$$

The scalar transport equation, governing the transport of tracer quantities, is given by:

$$\frac{\partial(H_z C)}{\partial t} + \frac{\partial(uH_z C)}{\partial x} + \frac{\partial(vH_z C)}{\partial y} + \frac{\partial(\Omega H_z C)}{\partial s} = -\frac{\partial}{\partial s}\left(\overline{c'w'} - \frac{v_\theta}{H_z}\frac{\partial C}{\partial s}\right) + C_{source} \quad (5)$$

where u, v, Ω are the average velocity components in the horizontal direction (x and y) and the vertical direction (s), the vertical coordinates of the sigma $s = (z - \eta)/D$ start from $s = -1$ at the base and $s = 0$ on the surface; z is a positive vertical coordinate with $z = 0$ at mean sea level; D is the total depth of sea water $D = h + \eta$, h is the depth below sea level from the sea floor; H_z is the thickness of the grid cell, f is the Coriolis parameter, p is the pressure, ρ and ρ_0 are the total density of sea water based on the reference, g is the gravitational acceleration, v and v_0 are the molecular viscosity and diffusivity, C shows the tracer quantity (example: temperature and salinity), C_{source} is the tracer source, and a function $\rho = f(C)$ is used to describe its density relationship.

The Reynolds stress parameters, which represent the turbulent fluxes of momentum and heat, are incorporated into the governing equations using the following relationships:

$$\overline{u'w'} = K_M\frac{\partial u}{\partial z}$$
$$\overline{v'w'} = K_M\frac{\partial v}{\partial z}$$
$$\overline{\rho'w'} = K_H\frac{\partial \rho}{\partial z} \quad (6)$$

where K_M is the eddy viscosity, representing the turbulent transport of momentum, and K_H is the eddy diffusivity, representing the turbulent transport of heat (Warner et al 2008).

The OpenDrift software was employed to model the trajectory of particles in the study area. The trajectory model utilizes an Eulerian-Lagrangian approach, where the hydrodynamic model's output, represented by velocity fields in Eulerian coordinates, is transformed into Lagrangian coordinates. Mathematically, the relationship between Lagrangian and Eulerian coordinates is derived from the velocity of a particle passing through a spatial domain (van Sebille et al 2018), $X(a,t) = x$ moving into the fluid velocity field at that point:

$$\left(\frac{\partial X(a,t)}{\partial t}\right)_a = v(x,t) \quad (7)$$

When a particle is located within a wet cell in the grid model, it is subjected to advection-diffusion processes at each time step. The Lagrangian trajectory $r_p(t)$ of the $p-th$ particle is calculated using the second-order Runge-Kutta method:

$$\frac{dr_p(t)}{r_p(0)} = u_c\big(r_p(t),t\big) + q.u_{w,p}\big(r_p(t),t\big) + u_s\big(r_p(t),t\big) + u'$$

where $r_p(0)$ represents the initial position of the $p-th$ particle, q is a scale factor for the drift velocity object, the term $u_c(r_p(t),t)$ denotes the Eulerian velocity at the particle's location $r_p(t)$ and time t, the term u' represents random fluctuations within the velocity vector.

Data input. Bathymetric data for the study was derived from extracted National Oceanic and Atmoshperic Administration (NOAA) grid data with a resolution of 1 km for the larger model domain (Figure 1a) and a resolution of 150 m for the smaller model domain (Figure 1b).

The initial conditions for temperature, salinity, and ocean currents in the larger model domain were obtained from the Hybrid Coordinate Ocean Model HYCOM + NCODA Global 1/12° Reanalysis. Afterwards, these spatially and temporally resolved data were then used as initial values and boundary conditions for the smaller model domain.

Tidal data were derived from the Tide Prediction and Observation Model (TPXO) harmonic tidal model, which utilizes sea level data observed by the Topex-Poseidon Satellite. The tidal components incorporated into the model simulations included M2, S2, N2, K2, K1, O1, P1, and Q1. To verify the model's performance, simulated results were compared against field observations of sea level tides obtained from the Geospatial Information Agency (BIG) tide gauge station at Sunda Kelapa, located at coordinates 6°07'00" S and 106°05'10" E.

Wind data were obtained from the European Centre for Medium-Range Weather Forecasts (ECMWF) and represents the 10-meter wind speed above the sea surface. This data was utilized as a forcing term in the model. Wind patterns follow the seasonal variations in the Java Sea. The average wind speed in June 2018 was 2.77 m s^{-1} from the southeast. Winds in November 2018 were relatively weak, with an average speed of 2.19 m s^{-1} and a direction ranging from northeast to southeast. Wind speeds between 0 and 2 m s^{-1} occurred 49.30% of the time, while speeds between 2 and 4 m s^{-1} occurred 40.29% of the time.

Rainfall data were also obtained from ECMWF and was used for bulk-fluxes formulation with a 3-hour time step. The amount of rainfall in the western Java Sea increases during the wet season, reaching its peak in March. Rainfall begins to decrease and reaches its lowest point in August. This indicates the influence of seasonal winds on Jakarta Bay.

River discharge data obtained from the Research and Development Center for Water Resources (Figure 2), Ministry of Public Works indicates that the Citarum and Cengkareng Rivers are the largest contributors of freshwater to Jakarta Bay, with

discharge rates of 100 $m^3 s^{-1}$ and 22.6 $m^3 s^{-1}$, respectively, in February. The highest discharge rate for the Cisadane River occurs in January, reaching 86.9 $m^3 s^{-1}$.

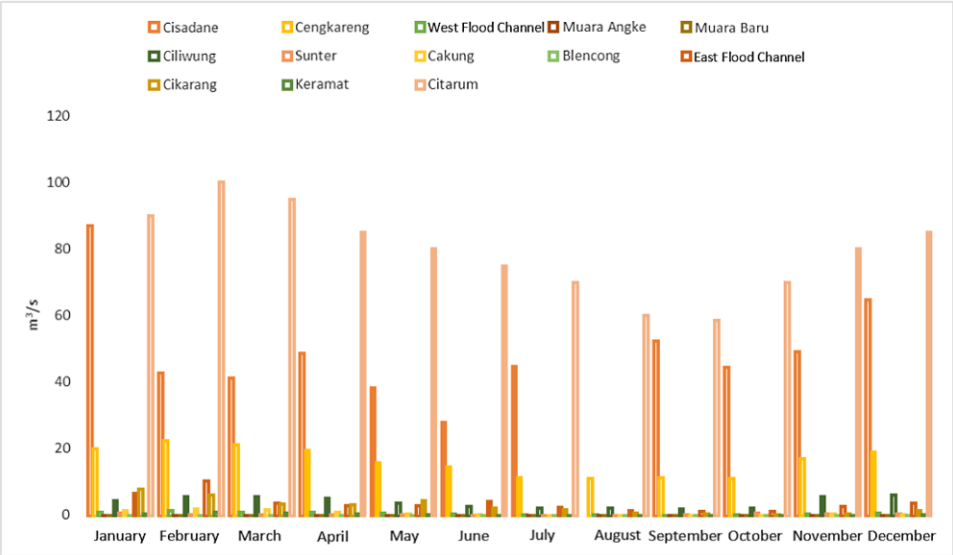

Figure 2. River Discharge into Jakarta Bay (Source: Research and Development Center for Water Resources).

Model setup. The larger domain area with spatial resolution of 1 km for hydrodynamic model was run in baroclinic mode with grid size of 207 x 250 x 15 with time step of 60 second. River discharge is not considered yet in this scenario. Meanwhile, smaller domain area with spatial resolution of 150 m was run with grid size of 346 x 480 x 10 with time step of 30 second. The model was run in baroclinic mode using timestep of 30 second and considering discharge from 13 rivers along the Jakarta Bay. Both simulations using parameters are given in Table 1.

Table 1

Parameters used in ROMS

Parameter	*Description*	*Value*	*Units*
TNU2	Nonlinear model lateral, harmonic, constant, mixing coefficient for active and inert tracer variables	50	$m^2 s^{-1}$
VISC2	Nonlinear model lateral, harmonic, constant, mixing coefficient for momentum	100	$m^2 s^{-1}$
AKT_BAK	Background vertical mixing coefficient for active and inert tracer variables	$1x10^{-6}$	$m^2 s^{-1}$
AKK_BAK	Background vertical mixing coefficient for turbulent kinetic energy	$5x10^{-6}$	$m^2 s^{-1}$
AKP_BAK	Background vertical mixing coefficient for turbulent generic statistical field	$5x10^{-6}$	$m^2 s^{-1}$
GLS_P	Stability exponent (nondimensional)	3	-
GLS_M	Turbulent kinetic energy exponent (nondimensional)	1.5	-
GLS_N	Turbulent length scale exponent (nondimensional)	-1	-
GLS_KMIN	Minimum value of specific turbulent kinetic energy	$7.6x10^{-6}$	-
GLS_PMIN	Minimum value of dissipation	$1x10^{-12}$	-
GLS_CMU0	Stability coefficient	0.5477	-
GLS_C1	Shear production coefficient	1.4	-
GLS_C2	Dissipation coefficient	1.92	-

GLS_C3M	Buoyancy production coefficient (minus)	-0.4	-
GLS_C3P	Buoyancy production coefficient (plus)	1	-
GLS_SIGK	Constant Schmidt number (nondimensional) for turbulent kinetic energy diffusivity	1	-
GLS_SIGP	Constant Schmidt number (nondimensional) for turbulent generic statistical field	1.3	-
RDRG	Linear bottom drag coefficient	$3x10^{-4}$	$m^2 s^{-1}$
RDRG2	Quadratic bottom drag coefficient	$3x10^{-3}$	-
Zob	Bottom roughness	0.02	m
Zos	Surface roughness	0.02	m
BLK_ZQ	Height of surface air humidity measurement (usually recorded at 10 m)	2	m
BLK_ZT	Height of surface air temperature measurement (usually recorded at 2 or 10 m)	2	m
BLK_ZW	Height of surface wind measurement (usually recorded at 10 m)	10	m

In the trajectory simulation, 100 kg-wet is assumed to represent one particle. Therefore, the number of particles released from each river mouth is based on the waste data presented in Table 2. For this study, marine debris is assumed to have a density lower than that of Jakarta Bay seawater, which is 1,027 kg m^{-3}. Based on this assumption, the positions of waste particles during the simulation (maximum of 1 month) are assumed to remain at the sea surface.

Table 2

Initial particle locations in the trajectory simulation for each month

River mouth	*Waste quantity (ton-wet)*	*Assumed particles*
Cisadane	0.6	6
Cengkareng	7.9	79
West Flood Channel	0.6	6
Angke River	0.6	6
Muara Baru	0.6	6
Ciliwung	0.6	6
Sunter	0.6	6
Cakung	0.6	6
Blencong	0.6	6
East Flood Channel	6.6	66
Cikarang	6.6	66
Keramat	6.6	66
Citarum	6.6	66

Source: Cordova & Nurhati (2019).

Model validation and performance analysis. To verify the hydrodynamic model's performance, simulated results were compared against field observations of sea level tides obtained from the Geospatial Information Agency (BIG) tide gauge station at Sunda Kelapa, located at coordinates 6°07'00" S and 106°05'10" E. Meanwhile particle movement was validated against drifter measurements. To assess the model's performance, the root mean squared error (RMSE) and mean absolute percentage error (MAPE) will be calculated for both tidal elevations and particle trajectories.

The RMSE is calculated by squaring the error (predicted minus observed) for each data point and then dividing by the total number of data points according to the following formula:

$$\text{RMSE} = \sqrt{\frac{1}{n}\sum_{i=1}^{n}(y_{obs_i} - y_{mod_i})^2} \qquad (9)$$

The mean absolute percentage error (MAPE) is calculated using the following formula:

$$\text{MAPE} = \frac{100}{n}\sum_{i=1}^{n}\frac{|y_{obs_i} - y_{mod_i}|}{y_{obs_i}} \qquad (10)$$

where n is number of data points, $observed_i$ is observed data value, and $predicted_i$ is model output data value.

Results and Discussion. Surface currents in the Java Sea exhibit distinct seasonal variations, transitioning from a westward flow during the eastern monsoon (July) to an eastward flow during the western monsoon season (January). This pattern is evident in the large-scale model results (Figure 3), where the average monthly surface currents for January (representing the western monsoon) show an eastward and northeasterly direction in the western Java Sea, while those for July (representing the eastern monsoon) exhibit a westward and southwesterly direction. During the transitional periods between the two monsoons, the surface currents in the western Java Sea tend to flow northward.

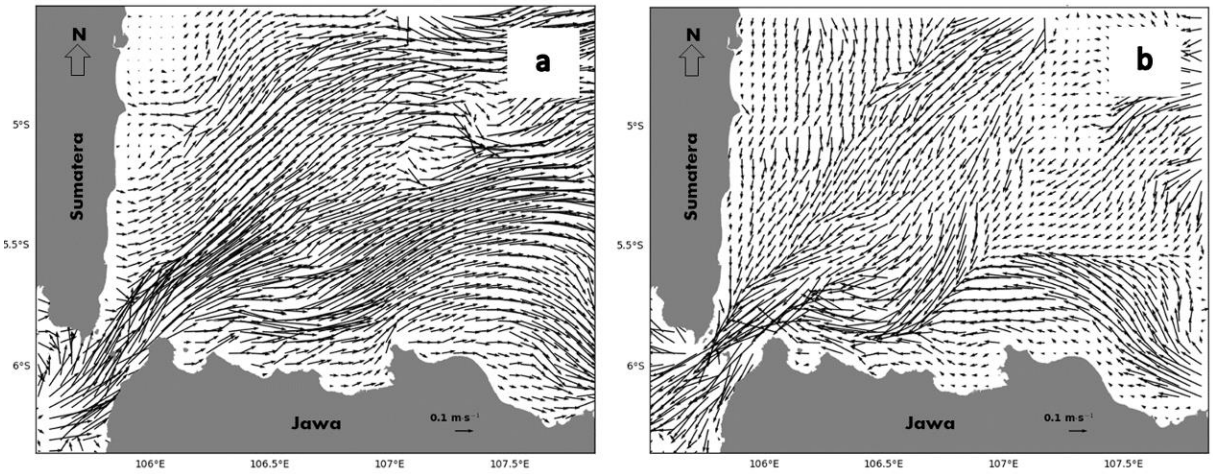

Figure 3. Average surface currents in (a) January and (b) July represent western and eastern monsoon respectively.

Particle movement validation. The model's particle movement was validated by comparing simulated particle trajectories with drifter measurements conducted south of Pari Island on November 10, 2018. The results show that the model captures the general pattern of particle movement (Figure 4). Drifters were released between 06:00 and 09:00 WIB. Both the drifter observations and the model trajectories indicated a westward movement from 06:00 to 07:00, with the model showing a slightly faster movement. From 08:00 to 09:00, both the drifter observations and the model trajectories exhibited a return movement towards the northeast. The distance difference between the model trajectory and the field data at 09:00 is approximately 300 meters. Overall, these results suggest that the employed model can effectively simulate the movement of surface marine debris.

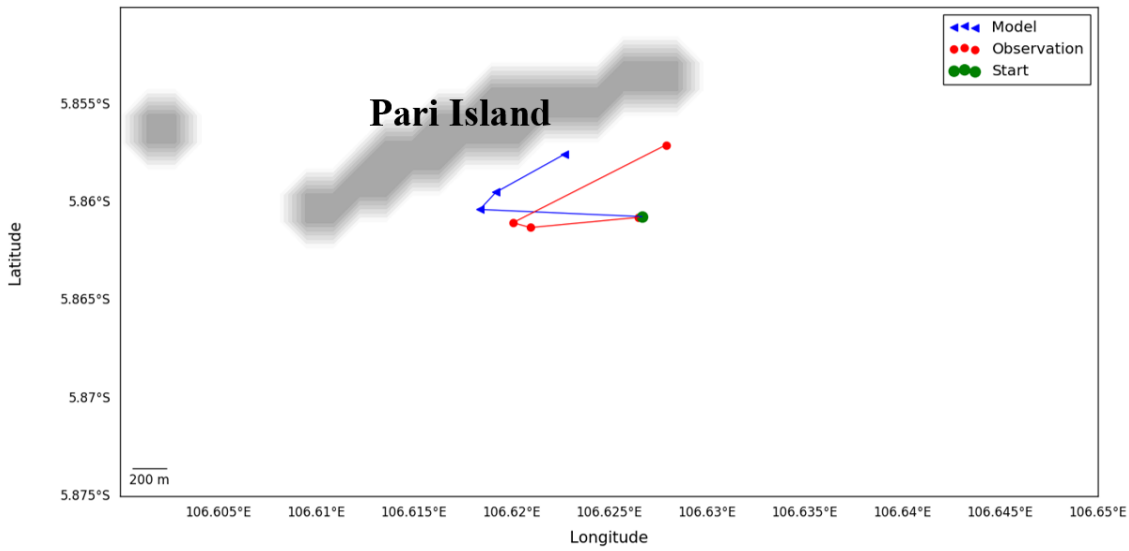

Figure 4. Particle movement patterns: model results (blue) and field observations (red).

Surface current patterns in Jakarta Bay and Seribu Island. The average monthly surface current speeds in the Java Sea exhibit a distinct seasonal pattern. During the western monsoon (represented by January 2018), the eastward and northeasterly currents reached their maximum average speed of 0.32 m s^{-1} in January (Figure 5). The direction of these surface currents shifted northward in March, with an average speed of 0.26 m s^{-1}.

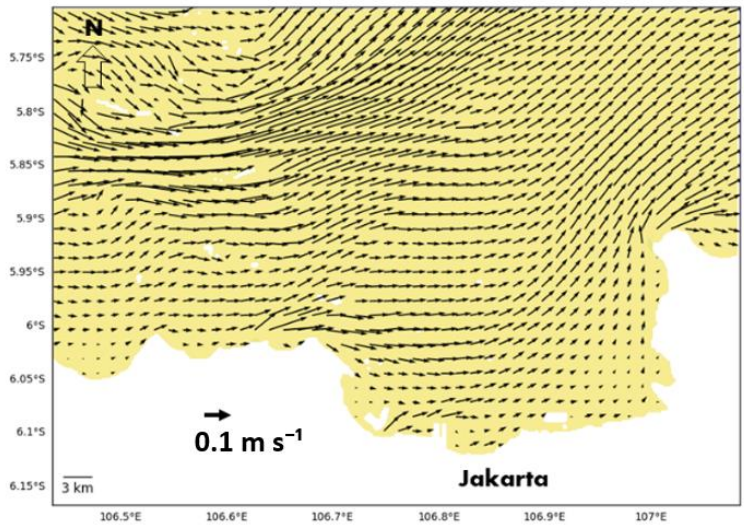

Figure 5. Average surface current speeds for January 2018.

The transition from the western to the eastern monsoon didn't involve an immediate shift in current direction from west to east. Instead, the dominant eastward flow gradually emerged in August 2018 (Figure 6).

In all seasons, surface current speeds were generally higher in the outer parts of Jakarta Bay compared to the inner bay. The difference in speed between the outer and inner bay was approximately 0.06 m s^{-1}. Additionally, due to the influence of river discharge, the currents near the mouths of the Cisadane and Citarum Rivers exhibited higher speeds compared to the surrounding areas, reaching 0.1 m s^{-1} and 0.04 m s^{-1}, respectively. This was particularly evident during the western monsoon when river discharge was at its highest (Figure 7).

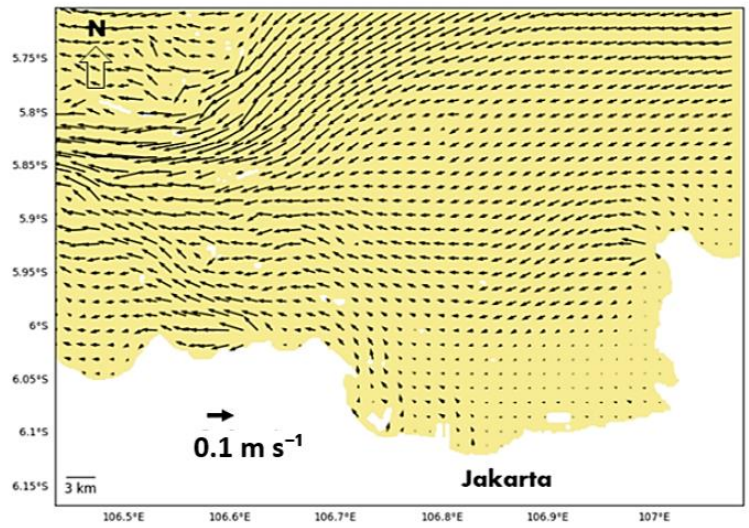

Figure 6. Average surface current speeds for August 2018.

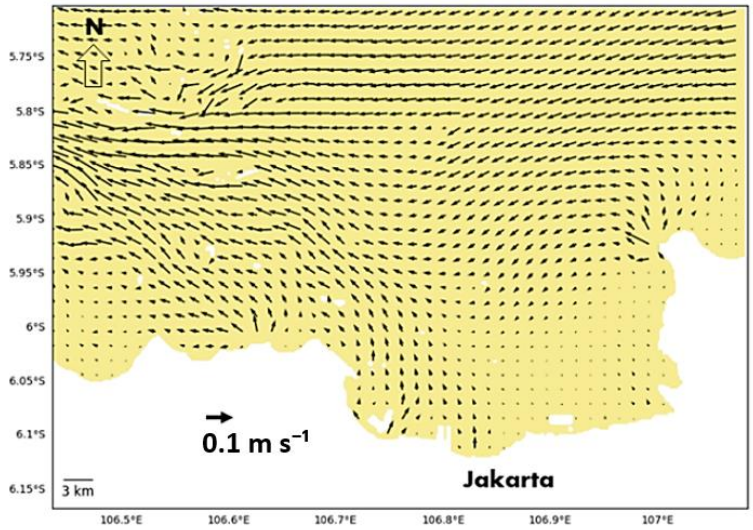

Figure 7. Average surface current speeds for November 2018.

Particle trajectories. To address the first research question, particle trajectory modeling was conducted for several days in early November 2018. The results indicate that debris originating from Cengkareng, West Flood Channel, and Muara Angke traveled 31 km northward towards the waters of Lancang Besar Island over a period of 6 days (Figure 8).

Debris from the Ciliwung River mouth traveled 36 km northward towards the waters of Lancang Besar Island over a period of 6 days. Debris from Cakung traveled 40 km seaward over a period of 13 days, reaching the waters north of Lancang Besar Island. Debris from Blencong traveled 42 km over a period of 12 days, reaching the waters north of Lancang Besar Island. Marine debris from East Flood Channel traveled 44 km southward towards the waters of Pari Island over a period of 12 days. Marine debris from Cikarang and Keramat traveled 43 km northward towards the waters of Lancang Besar Island over a period of 12 days. Debris originating from the Citarum River traveled 42 km over a period of 3-5 days, reaching the waters both south and north of Pari Island.

The particle trajectory model simulations suggest that the debris particles observed on November 2, 2018, originated from the Citarum River (Figure 9). These particles were able to move rapidly at an average speed of 0.15 m s^{-1} westward due to the strong currents generated by the Citarum River discharge, reaching the waters of Pari Island within 3 days.

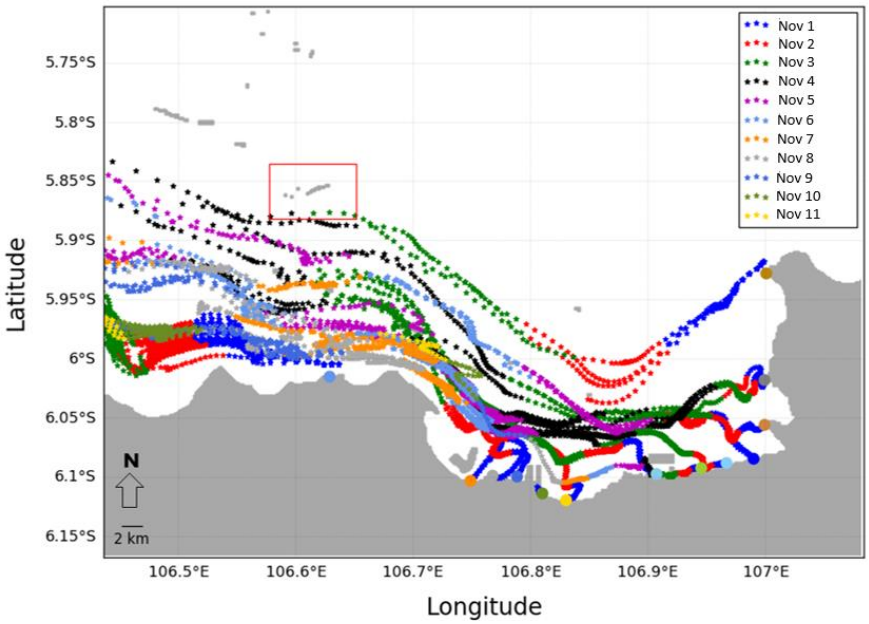

Figure 8. Particle trajectories for November 2018.

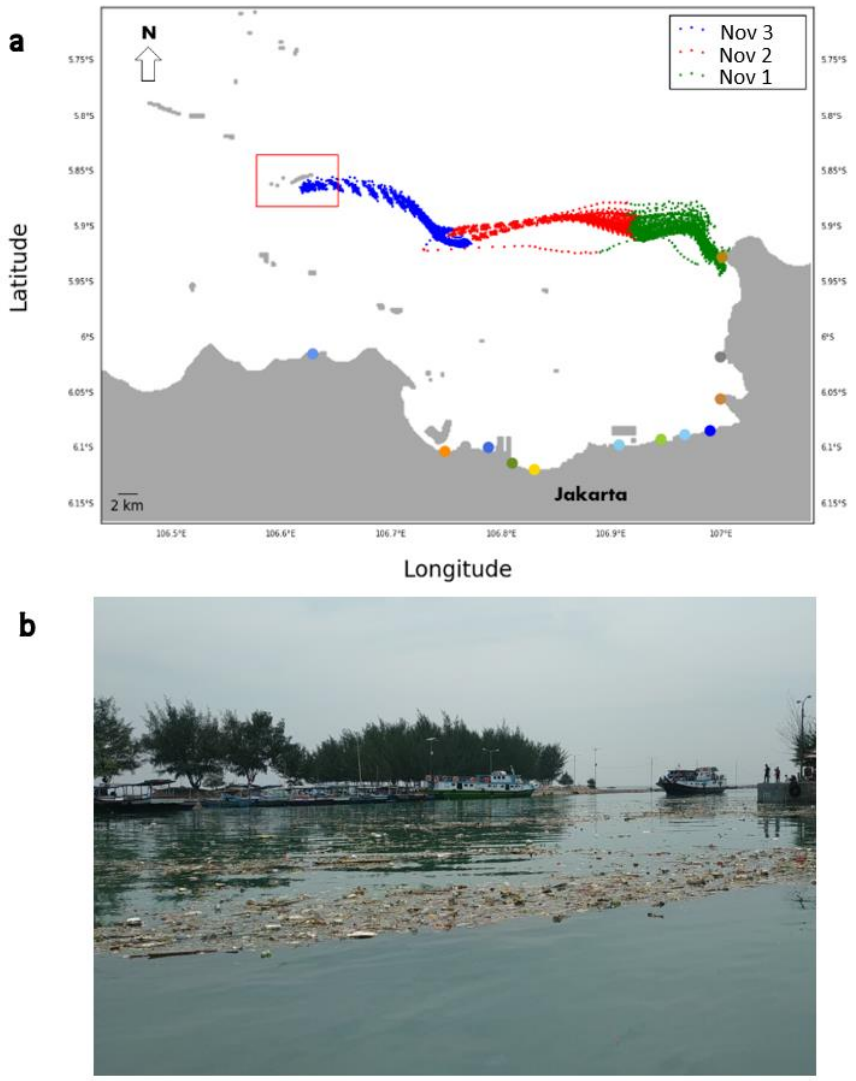

Figure 9. (a) Model trajectory results for November 1-3, 2018; (b) picture of debris distribution on November 3, 2018, at Pari Island.

Stranded particle analysis. To predict the sources of stranded debris in Seribu Island, particle trajectory simulations were conducted at the beginning of each month throughout 2018. The simulation results indicate that in January, no debris was stranded on Pramuka Island, Lancang Besar Island, Tidung Besar Island, Pari Island, or Bidadari Island. Only a small amount of debris was found on Untung Jawa Island. In February, marine debris was only observed on Lancang Besar Island and Untung Jawa Island, while no debris was found on Pramuka Island, Tidung Besar Island, Pari Island, or Bidadari Island.

During April and May, the islands closer to Jakarta Bay, such as Pari Island, Lancang Besar Island, Untung Jawa Island, and Bidadari Island, continued to receive debris from Jakarta. However, the more distant islands, such as Tidung Besar Island and Pramuka Island, did not receive any debris.

As the eastern monsoon approached, with its corresponding surface current patterns, most of the islands in Seribu Island received debris from Jakarta Bay. During the transition period from the eastern to the western monsoon, in October, November, and December, marine debris was stranded on all observed islands.

Based on the simulated stranded debris quantities from the 33,653 tons of debris released throughout 2018, Pramuka Island received debris from Cengkareng in November and December, amounting to 0.6 and 2.6 tons, respectively. Debris from the Sunter River mouth is estimated to have reached 0.6 tons on Pramuka Island. In total, during 2018, Pramuka Island was exposed to debris from Jakarta's river mouths to the extent of 5.2 tons or 0.015% of all debris discharged from the 13 river mouths in Jakarta Bay (Figure 10).

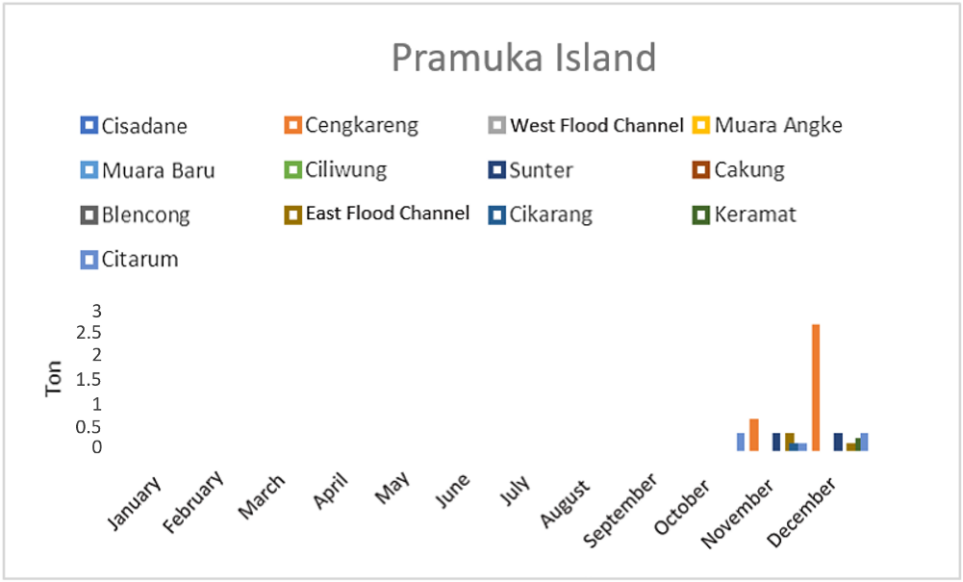

Figure 10. The monthly weight of stranded debris (in ton) at Pramuka Island.

Tidung Besar Island (Figure 11) received the largest amount of debris from Jakarta Bay in November, with details as follows: 0.3 tons from Cisadane, 7.5 tons from Cengkareng, 0.3 tons from Ciliwung and West Flood Channel, 7.6 tons from East Flood Channel, 1.2 tons from Cikarang, 0.6 tons from Keramat, and 0.5 tons from Citarum. The total stranded debris for Tidung Besar Island during 2018 amounted to 28.7 tons or 0.085% of the total debris discharged from the 13 river mouths in Jakarta. The absence of stranded debris in April, May, July, August, September, and October was attributed to the southward currents around Tidung Besar Island, which quickly moved westward, preventing debris from reaching the island. The average current speed south of Tidung Besar Island in April, May, July, August, September, and October ranged from 0.3 to 0.4 m s^{-1} westward, higher than in other months.

Figure 11. The monthly weight of stranded debris (in ton) at Tidung Besar Island.

Pari Island (Figure 12) also received the highest amount of debris from Jakarta Bay in November. During 2018, the total stranded debris on Pari Island amounted to 16.8 tons, representing 0.045% of the total debris released from Jakarta's river mouths. The Citarum River is estimated to be the largest contributor of debris to Pari Island during 2018. Considering Pari Island's geographical position, it is evident that a significant amount of debris from the Citarum River reaches the island due to its location directly west of the Citarum River (at approximately the same latitude).

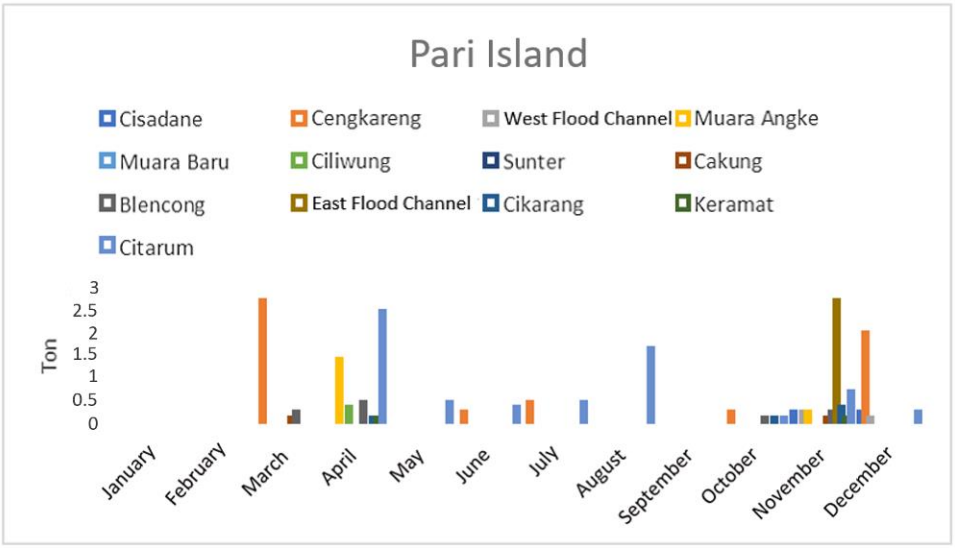

Figure 12. The monthly weight of stranded debris (in ton) at Pari Island.

Untung Jawa Island (Figure 13) received the highest amount of debris in July, with a total of 29.6 tons. Based on the sources, Cengkareng River is estimated to be the biggest polluter during 2018, with a total of 107.3 tons, followed by East Flood Channel with 43.6 tons. The large amount of debris from Cengkareng River was attributed not only to its proximity to Untung Jawa Island but also to its status as the largest source of debris among the rivers discharging into Jakarta Bay.

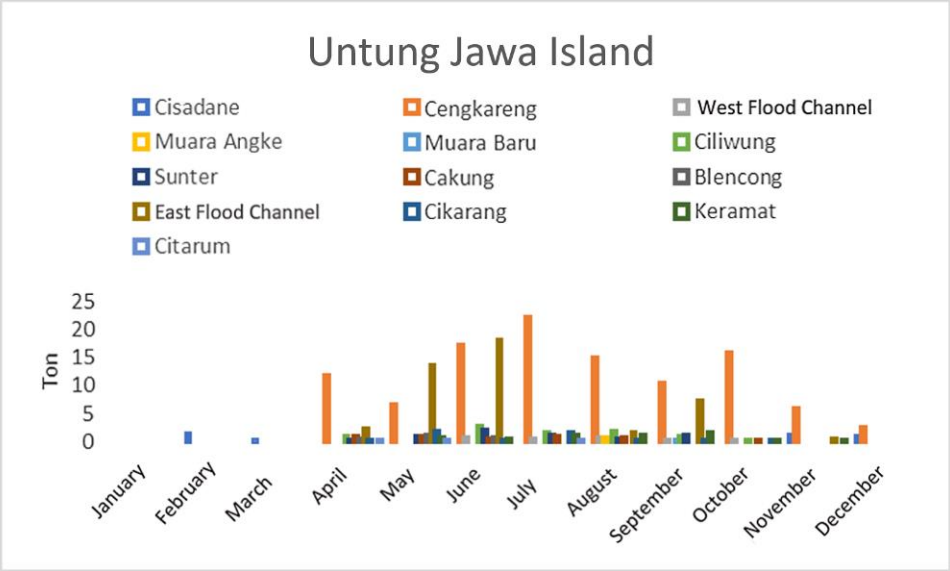

Figure 13. The monthly weight of stranded debris (in ton) at Untung Jawa Island.

A comparison of the stranded debris quantities among the four islands in Jakarta Bay reveals a decreasing trend from Bidadari Island (closest to Jakarta) to Pramuka Island (further north). This pattern could be primarily attributed to the prevailing westward currents during the eastern monsoon, which prevent marine debris originating from Jakarta Bay from reaching the northern parts of Untung Jawa Island and Lancang Besar Island.

Furthermore, the significant amount of marine debris stranded on Seribu Island could be largely attributed to the Cengkareng River. This was not only due to the higher volume of debris generated by the Cengkareng River but also due to its wider channel and greater discharge compared to other rivers discharging into Jakarta Bay.

Conclusions. The study confirms that a substantial amount of marine debris affecting Seribu Island originates from the Cengkareng River. This finding is supported by the river's higher debris volume, wider channel, and greater discharge compared to other rivers flowing into Jakarta Bay. Among the islands of Seribu Island, Untung Jawa Island recorded the highest accumulation of stranded marine debris, totaling 221 tons. This accumulation can be attributed to the island's position within the trajectory of debris exiting Jakarta Bay from April to December.

The seasonal influence on debris patterns is evident, particularly on Pramuka Island and Pari Island. Debris was predominantly stranded on Pramuka Island during October, November, and December, corresponding to transition period II into the western monsoon. Similarly, Tidung Besar Island experienced debris accumulation during transition periods I and II. In contrast, Pari Island saw an increase in stranded debris during transition periods, indicating a direct correlation with seasonal wind patterns affecting surface currents.

These observations mirror the findings of the hydrodynamic and trajectory modeling discussed in the study, highlighting the critical role of seasonal variations in marine debris distribution within Jakarta Bay and emphasizing the urgent need for targeted conservation strategies and legislative measures to address marine debris pollution and protect the sensitive aquatic ecosystems of Seribu Island.

Acknowledgements. This study was made possible by the support of the project titled "Marine Macro- and Micro-Plastic Analysis and their distribution in the North Coast of Java During the Recent Time [FITB.MTCRC-1-03-2023]".

Conflict of interest. The authors declare that there is no conflict of interest.

References

Cordova M. R., Nurhati I. S., 2019 Major sources and monthly variations in the release of land-derived marine debris from the Greater Jakarta area, Indonesia. Scientific Reports 9:18730.

Chassignet E. P., Arango H., Dietrich D., Ezer T., Ghil M., Haidvogel D. B., Ma C. C., Mehra A., Paiva A. M., Sirkes Z., 2000 DAMEE-NAB: the base experiments. Dynamics of Atmospheres and Oceans 32(3-4):155-183.

Diastomo H., Surya M. Y., Sakti A. D., Agustina E., Trismadi, 2021 Marine debris tracking from river discharge base on hydrodynamic simulation on Jakarta Bay. IOP Conference Series: Earth and Environmental Science 925(1):012005.

Haidvogel D. B., Beckmann A., 1999 Numerical ocean circulation modeling. Imperial College Press, London, 344 pp.

Kisnarti E. A., Ningsih N. S., Putri M. R., Hendiarti N., Mayer B., 2024 Dispersion of surface floating plastic marine debris from Indonesian waters using hydrodynamic and trajectory models. Marine Pollution Bulletin 198:115779.

Mayer B., Pohlmann T., 2014 Simulation of organic pollutants: first step towards an adaptation to the Malacca Strait. Asian Journal of Water, Environment and Pollution 11(1):75-86.

Mulia D., 2004 [Alternative development of Pari Islands cluster in Seribu Islands as an ecotourism marine object in DKI Jakarta]. BSc thesis, Aquatic Resources Management Study Program, Faculty of Fisheries and Marine Science – Institut Pertanian Bogor, Bogor, 149 pp. [in Indonesian]

Putri M. R., 2005 Study of ocean climate variability (1959-2002) in the Eastern Indian Ocean, Java Sea and Sunda Strait using the HAMburg shelf ocean model. Doctoral dissertation, Staats-und Universitätsbibliothek Hamburg Carl von Ossietzky, 104 pp.

Putri M. R., Pohlmann T., 2014 Lagrangian model simulation of passive tracer dispersion in the Siak Estuary and Malaca Strait. Asian Journal of Water, Environment and Pollution 11(1):67-74.

Rahman L., Zamani N. P., Ismet M. S., Cordova M. R., 2024 Effects of seasonal variation on the characteristics of stranded marine debris within Rambut Island Wildlife Reserve, Indonesia. Jurnal Kelautan Tropis 27(1):129-138.

Shchepetkin A. F., McWilliams J. C., 2005 The regional oceanic modeling system (ROMS): a split-explicit, free-surface, topography-following-coordinate oceanic model. Ocean Modelling 9(4):347-404.

Tsani R. N., 2017 [Two-dimensional horizontal particle trajectory model in Pari Island - Seribu Islands]. BSc thesis, Oceanography Study Program, Faculty of Earth Sciences and Technology – Institut Teknologi Bandung, Bandung, 58 pp. [in Indonesian]

van Sebille E. V., Griffies S. M., Abernathey R., Adams T. P., Berloff P., et al, 2018 Lagrangian ocean analysis: fundamentals and practices. Ocean Modelling 121:49-75.

Warner J. C., Sherwood C. R., Signell R. P., Harris C. K., Arango H. G., 2008 Development of a three-dimensional, regional, coupled wave, current, and sediment transport model. Computers and Geosciences 34(10):1284-1306.

Wicaksono B., Tiaraningrum, Ilmi F., Cholifatullah F., Hasan S., Saribanon N., 2022 Coastal biodiversity of Tidung and Rambut Islands: mangrove and coral reef conservation program. Journal of Tropical Biodiversity 3(1):28-42.

Widyayanto H. S., Helmi M., Munasik, Wouthuyzen S., 2009 Determination of coral reef ecosystem vulnerability index using cell-based spatial modeling in the Pari Islands Cluster, Seribu Island. Globe 11(2):88-96.

World Bank Group, 2018 Indonesia marine debris hotspot. Synthesis report. 42 pp.

Received: 14 June 2024. Accepted: 05 July 2024. Published online: 11 July 2024.
Authors:
Mutiara Rachmat Putri, Research Group of Environmental and Applied Oceanography, Faculty of Earth Sciences and Technology, Bandung Institute of Technology, Ganesha Street, No. 10, 40132 Bandung, West Java, Indonesia; Study Program of Earth Science, Faculty of Earth Sciences and Technology, Bandung Institute of Technology, Ganesha Street, No. 10, 40132 Bandung, West Java, Indonesia, e-mail: mutiara.putri@itb.ac.id
Muhammad Riza, Study Program of Earth Science, Faculty of Earth Sciences and Technology, Bandung Institute of Technology, Ganesha Street, No. 10, 40132 Bandung, West Java, Indonesia, e-mail: rizaa34@gmail.com
Naffisa Adyan Fekranie, Research Group of Environmental and Applied Oceanography, Faculty of Earth Sciences and Technology, Bandung Institute of Technology, Ganesha Street, No. 10, 40132 Bandung, West Java, Indonesia, e-mail: academicnaffisa@gmail.com
Agus Setiawan, Research Centre for Deep Sea, Research Organisation for Earth Sciences and Maritime, National Research and Innovation Agency, M.H. Thamrin No. 8, 10340, Central Jakarta, Indonesia, e-mail: agus185@brin.go.id
Hansan Park, Korea-Indonesia Marine Technology Cooperation Research Center (MTCRC), M.H. Thamrin No. 8, 10340, Central Jakarta, Indonesia, e-mail: hansanpark@mtcrc.center
This is an open-access article distributed under the terms of the Creative Commons Attribution License, which permits unrestricted use, distribution and reproduction in any medium, provided the original author and source are credited.
How to cite this article:
Putri M. R., Riza M., Fekranie N. A., Setiawan A., Park H., 2024 Numerical modeling of debris trajectory in Jakarta Bay: assessing the threat to Seribu Island. AACL Bioflux 17(4):1323-1338.